Enzyme Inhibition

DOI: 10.1002/ange.201311114

The Bioinorganic Chemistry of Apoptosis: Potential Inhibitory Zinc Binding Sites in Caspase-3**

*A. Gerard Daniel, Erica J. Peterson, and Nicholas P. Farrell**

Abstract: *Zn^{2+} inhibits the action of several of the caspases and thus may act as a regulator of apoptosis. Reversal of this inhibition is one possible approach for the development of apoptosis-based therapies. Few studies describe the molecular details of the Zn^{2+}–caspase interaction, the understanding of which is essential for the success of any therapeutic strategies. Enzyme kinetics and biophysical studies have shown that the inhibition is of mixed type with prominent (ca. 60% of inhibition) uncompetitive characteristics and an IC_{50} of 0.8 μM under the conditions used. Fluorescence-based techniques confirmed that, during inhibition in the sub-micromolar range, substrate binding remains unaffected. A new zinc binding site composed of the catalytic histidine and a nearby methionine residue, rather than the catalytic histidine and cysteine dyad, is proposed based on the experimental observations. DFT models were used to demonstrate that the proposed site could be the preferred inhibitory zinc binding site.*

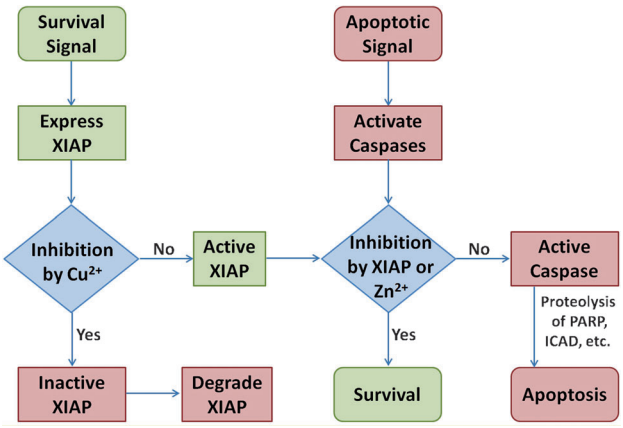

Figure 1. The regulation of apoptosis by Cu^{2+} and Zn^{2+}. Processes that favor survival are shaded green, and those favoring apoptosis are shaded red. Regulatory processes are shaded blue.

Central to the process of apoptosis, an integral part of cellular homeostasis in multicellular organisms, are the cysteine-dependent aspartate-specific proteases (caspases).[1] The endogenous metal ions $Cu^{+/2+}$ and Zn^{2+} play important roles in the apoptotic pathway (Figure 1).[2,3] Zn^{2+} inhibits the action of caspases-3, 6, 7, 8 and 9.[4] This fascinating aspect of Zn^{2+} adds a dynamic regulatory role in cellular processes to its well-defined catalytic and structural functions.[2,5] The molecular details of this inhibition, crucial for the development of caspase-targeted therapies, are scarce. Discrete inhibitory sites for caspase-9[4c] and caspase-6, determined by X-ray crystallography, have been described.[6] The inhibitory sites of caspases-3, 7 and 8 remain to be characterized. Based on enzyme kinetics, biophysical studies, and DFT models, we propose a zinc binding site specific to caspases-3 and 7 that consists of the essential His of the catalytic dyad (His121 and Cys163) and a nearby Met residue, rather than the cysteine thiolate. More than one zinc inhibition site is present.

The catalytic dyad is suggested to be the common inhibitory zinc binding site for all caspases.[4a,c,5b,6] The presence of only two strongly-binding protein residues differentiates the inhibitory zinc sites from the more common 3- and 4-coordinate sites associated with catalytic and structural Zn^{2+}, respectively. A formally "two-coordinate" binding site may allow the dynamic reversibility required for a regulatory role, but a weakly bound Zn^{2+} may not effectively compete against the substrate at the active site. Hence, we performed systematic enzyme kinetics to determine the details of the Zn^{2+} inhibition of caspase-3. We used a minimal buffer to avoid interference from reducing and chelating agents (see the Supporting Information). A mixed-model equation provided the overall best fit for the Michaelis–Menten plot (Figure 2a). Under the conditions used, the IC_{50} of Zn^{2+} towards caspase-3 is 0.8 μM. Considering possible Zn–Tris interactions, the actual IC_{50} could be as low as 40 nM (Tris = tris(hydroxymethyl)aminomethane in the buffer; see the Supporting Information). In the 0.4 to 1.4 μM range, V_{max}^{app} decreases with increasing $[Zn^{2+}]$ (Figure 2b), thus indicating a mechanism other than competitive inhibition. The complexity involved in the inhibition can also be seen from the Lineweaver–Burk plot, (Figure 2c). The K_m^{app} value seemingly decreases up to 1 μM $[Zn^{2+}]$ but increases above this concentration. Although the change in K_m^{app} is not large, this reproducible trend indicates a sudden change in the mode of inhibition. The initial decrease in K_m^{app}, along with a steady decrease in V_{max}^{app}, resembles uncompetitive inhibition (Figure 2b). The initial higher value of K_i compared to K_i' is also supportive of uncompetitive inhibition, thus suggesting

[*] A. G. Daniel, Dr. N. P. Farrell
Department of Chemistry, Virginia Commonwealth University
Richmond, VA 23284 (USA)
E-mail: npfarrell@vcu.edu
A. G. Daniel, E. J. Peterson, Dr. N. P. Farrell
Massey Cancer Center, Virginia Commonwealth University
Richmond, VA 23294 (USA)

[**] This work was supported by VCU Presidential Research Quest Fund. A.G.D. is grateful to the Altria Group, Inc. for their support through a fellowship. We are thankful to Dr. Guy Salvesen for the plasmid.
Supporting information for this article is available on the WWW under http://dx.doi.org/10.1002/anie.201311114.

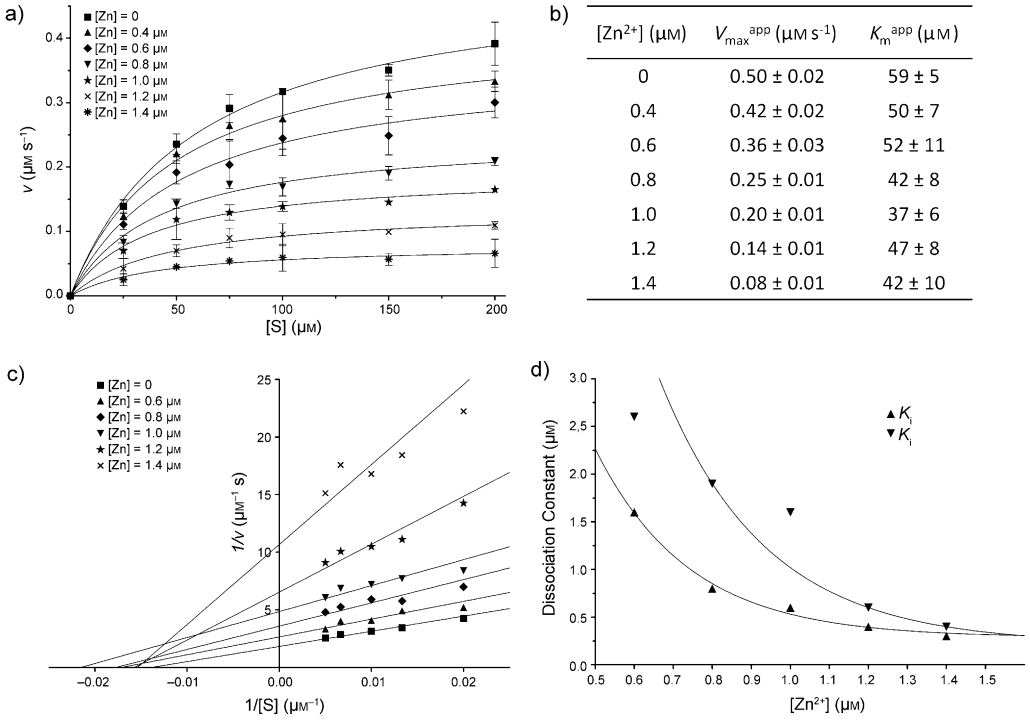

$[Zn^{2+}]$ (μM)	V_{max}^{app} (μM s^{-1})	K_m^{app} (μM)
0	0.50 ± 0.02	59 ± 5
0.4	0.42 ± 0.02	50 ± 7
0.6	0.36 ± 0.03	52 ± 11
0.8	0.25 ± 0.01	42 ± 8
1.0	0.20 ± 0.01	37 ± 6
1.2	0.14 ± 0.01	47 ± 8
1.4	0.08 ± 0.01	42 ± 10

Figure 2. Kinetic analyses of caspase-3 inhibition for 0–1.4 μM Zn^{2+}. a) Michaelis–Menten plot fitted using a mixed inhibition model equation. b) Kinetic parameters obtained from the fitting of the Michaelis–Menten plot. c) Lineweaver–Burk plot with linear fitting. d) Plot of K_i and K_i' vs $[Zn^{2+}]$.

unperturbed binding of the substrate to the active site in the presence of Zn^{2+} (Figure 2d). With increasing $[Zn^{2+}]$, the K_i value decreases and attains equality to K_i', thus implying a transition towards noncompetitive inhibition. From this analysis, we suggest the existence of more than one zinc binding site in caspase-3, an idea consistent with previous reports.[6]

The changes in substrate binding affinity of caspase-3 in the presence of Zn^{2+} were examined by fluorescence polarization (FP) by using a fluorescently-labelled tetrapeptide irreversible inhibitor (FITC-C6-DEVD-fmk) as a substrate mimic. Substrate binding to the enzyme was not affected up to 1 μM Zn^{2+}, after which the binding decreased significantly, thus confirming the previous trends (Figure 3). The increase in polarization seen at 5 and 10 μM Zn^{2+} may be due to nonspecific interactions because the enzyme is totally inactive at these higher concentrations.

The perturbation of caspase-3 as a result of substrate binding can be monitored from changes in the fluorescence of the two Trp residues close to the active site (Figure 4a).[7] The addition of Zn^{2+} quenches the fluorescence of caspase-3 in a concentration-dependent manner (Figure 4b). Up to 2 μM of Zn^{2+}, a small blue shift and a decrease in fluorescence with band narrowing was observed. At 3 μM, however, a larger blue shift accompanied a decrease in fluorescence with band broadening. Above 3 μM, the band broadened further with a small blue shift and intensity increase. Again, these results indicate the existence of more than one zinc binding site with different binding affinities. In the presence of the reversible inhibitor Ac-DEVD-CHO and 1 μM Zn^{2+}, caspase-3 fluorescence significantly decreased, a result that can be attributed to additive quenching from both inhibitors (Figure 4c,d). Above 1 μM, the spectra were comparable to those measured in the absence of peptide, thus implying that most of the quenching is due to Zn^{2+}, a result that confirms that reduced substrate binding only occurs at higher zinc concentrations.

In summary, more than 50% inhibition occurs in the sub-micromolar range, but substrate binding to caspase-3 is not affected by Zn^{2+} at these concentrations. These experiments suggest the existence of more than one zinc binding site. From the fluorescence studies, it is evident that Zn^{2+} affects the active site environment but does not induce any noticeable change in the secondary structure of caspase-3, as confirmed by CD spectroscopy (Figure S1 in the Supporting Information).

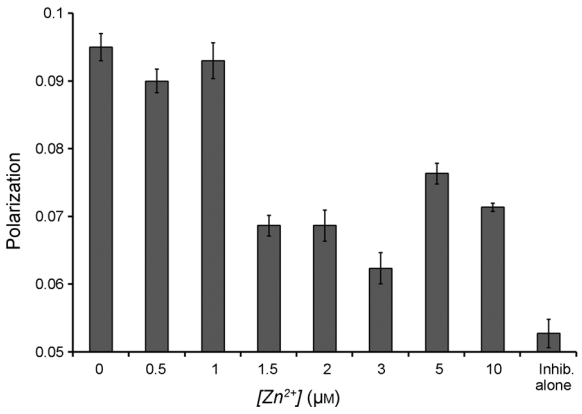

Figure 3. The influence of Zn^{2+} on substrate binding to caspase-3, monitored by using the fluorescence polarization resulting from the fluorescein isothiocyanate (FITC)-tagged caspase-3 inhibitor FITC-C6-DEVD-fmk. The inhibitor alone, without caspase-3, was also measured as a control.

The proposed mechanism of caspase proteolysis involves sequential steps of substrate recognition and binding at the active site, followed by nucleophilic attack on the substrate aspartate carbonyl by the catalytic thiolate, thereby leading to a thioester intermediate. Histidine assists in hydrolyzing the thioester, thereby leading to the product and closing the catalytic cycle (Figure S2). Substrate binding at the active site

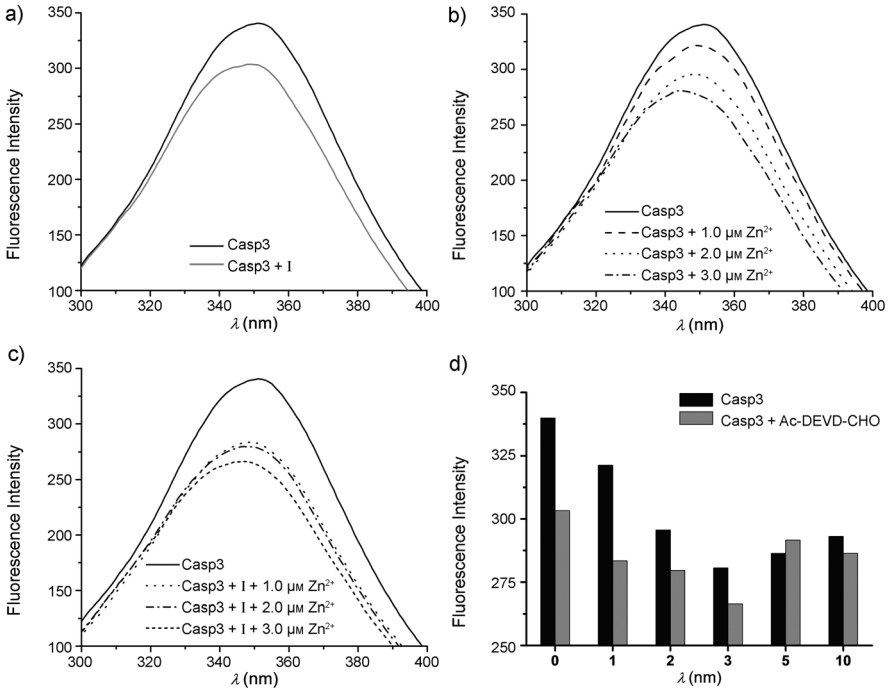

Figure 4. Fluorescence spectra showing the intrinsic fluorescence of caspase-3 under various conditions. a) Fluorescence quenching of caspase-3 by Ac-DEVD-CHO (I) used as substrate mimic. b) Fluorescence quenching of caspase-3 in the presence of 1–3 μM Zn^{2+} c) Fluorescence quenching of caspase-3 in the presence of Ac-DEVD-CHO and 1-3 μM Zn^{2+}. d) Fluorescence intensity at the λ_{max} of caspase-3, with or without a reversible inhibitor, under the influence of various Zn^{2+} concentrations.

results in steric constraints, which render the binding of Zn^{2+} to Cys163 unlikely. An alternative mechanism of inhibition must therefore consider the effects of Zn^{2+} on the function of His121. Investigation of the caspase-3 crystal structures shows a potential Zn-binding ligand, Met61, in close proximity to His121 (Figure S3). The Met residue is part of a hydrophobic recess, formed along with Phe55 and Phe128, which harbors His121. Any change in these residues affects the activity of the enzyme (Figure S4).

Methionine is not a common ligand in zinc proteins but it is confirmed to bind in Zn^{2+}-substituted cytochrome c.[8] Moreover, divalent S acts as a Zn^{2+} ligand in several model compounds.[9] Accordingly, we performed DFT modeling of potential zinc binding sites for the cystein–histadine catalytic dyad (Zn**CH**) and for Met61 and His121 (Zn**MH**; Figure 5a,b; see the Supporting Information for details). The optimized geometries in both cases resemble a distorted tetrahedron (Table S1 in the Supporting Information). The Zn**CH** site was more distorted, with a Zn–S bond length (*l*) of 2.438 Å and a S–Zn–N angle (∡) of 126.6°. Zinc bound to His and two water molecules with *l*(Zn–N) of 1.963 Å, and *l*(Zn–O) of 2.053 Å and 2.063 Å. For the Zn**MH** site, *l*(Zn–S) and *l*(Zn–N) were 2.307 and 1.946 Å, respectively, and ∡S–Zn–N was 119.8°. Moreover, the Zn**MH** site was 11.0 kcal mol^{-1} more stable than the Zn**CH** site. Notably, in the Zn**CH** site, the length of C_β–S bond of Cys163 is 1.872 Å, which is longer than normal. This might be an artifact resulting from fixing of the positions of the hydrogens on the α-carbon atoms. However, a longer C–S bond has been observed in a strained system.[10] Reoptimization of the Zn**CH** site with the hydrogens on the α-carbon atoms of Cys163 released resulted in a better geometry. Notably, *l*(Zn–S) measured 2.385 Å, the C_β–S bond of Cys163 was 1.841 Å in length, and the ∡S–Zn–N was 119.2°. Consequently, the system was stabilized by 8.7 kcal mol^{-1} compared to the original Zn**CH** site. This result suggests that backbone rearrangement would be needed for Zn^{2+} to bind tightly to the catalytic dyad. Although backbone movement occurs during metal coordination in some proteins,[11] it may not be favored in the case of the catalytic Cys of active caspases because this residue is locked in place by a cation–π interaction between an Arg and a Tyr residue and several H-bonding interactions along the L2 loop (Figure S5). Similarly, the catalytic His, which is part of a β-turn, is also rigid. However, the Met residue has a long side chain and is part of the L1 loop, which is comparatively flexible, so this residue would offer the plasticity required for metal binding (Figure S6). These considerations, along with the observed trends in energy and geometric parameters, leads us to conclude that the Zn**MH** site is favored over the Zn**CH** site for zinc binding.

Considering the Zn**MH** site as inhibitory explains the experimental observations. Firstly, zinc binding induces an approximately 90° rotation around the C_β–C_γ bond of the His residue, thereby flipping the imidazole ring away from the substrate binding groove. This conformational change is facilitated by the favorable σ–π interaction between a zinc-bound water molecule, the methyl group on Met61, and Phe128. Consequently, the substrate binding groove expands. This may increase the substrate binding affinity by reducing steric hindrance as can be seen from the trends in the K_m^{app} values. Given that this site is distant from the Trp residues, the fluorescence change of caspase-3 with Zn^{2+} may be due to changes in the solvation environment. Mechanistically, since His121 is no longer capable of acting as a general acid or base in its zinc-bound state, the inhibition is more likely to occur at the thioester intermediate stage (Figure S2) of the catalytic cycle, in which the His residue plays a role. In light of these rationales, the Zn**MH** site accounts for the observed uncompetitive-like inhibition of caspase-3.

Met61 is common to caspase-3 and caspase-7 (Met84) and is partially conserved as Leu or Ile in all other caspases (Figure S7). Given the high homology of caspase-7 to caspase-3, zinc inhibition of caspase-7 may follow similar kinetics, whereas caspases-6, 8 and 9 may differ as a result of the lack of a coordinating ligand in the place of Met61. The similarities and variability among caspases could be exploited to delineate the inhibitory zinc sites by comparative studies under

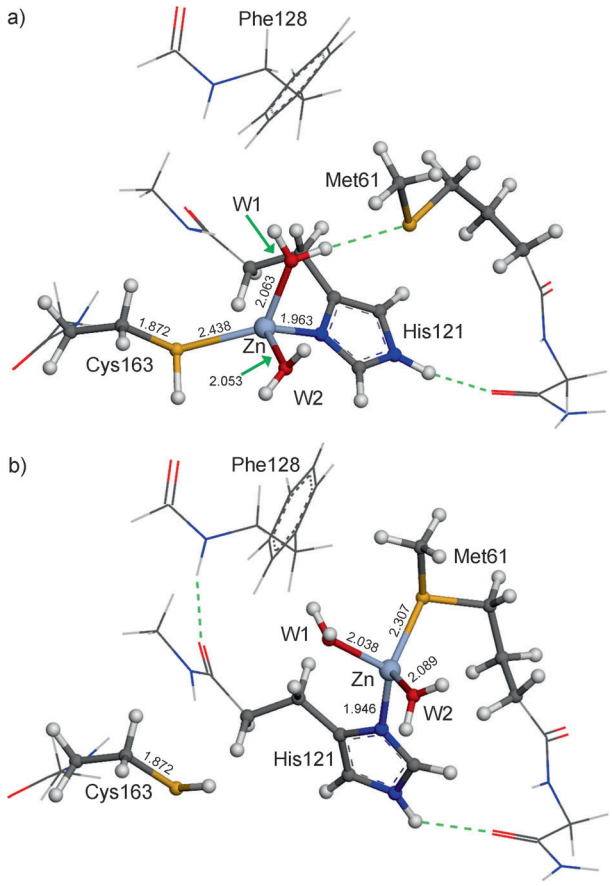

Figure 5. Optimized structures of probable zinc binding sites in caspase-3: a) the catalytic dyad (Zn**CH**) and b) His121 and Met61 (Zn**MH**). Zinc–ligand bond lengths (Å) are shown. W1 and W2 are water molecules.

identical conditions. The choice of conditions compatible with Zn^{2+} is critical, as emphasized elsewhere.[5b] For example, since the inhibitory sites are of low binding affinity, the existence of two modes of inhibition in caspase-3 may never be observable under the influence of even a weakly chelating agent such as β-mercaptoethanol.

The relevance of low-binding-affinity zinc sites such as the one described herein is highly debated. However, binding affinities in the low nanomolar range may be physiologically relevant.[2,5b] These findings have implications for the role of Zn^{2+} in apoptosis as well as for drug development. Firstly, targeted chelation of Zn^{2+} or Cu^{2+} is a strategy for regulating apoptosis. For example, procaspase-activating compound 1 (PAC-1) induces apoptosis in cancer cells by activating procaspase-3 and -7 through Zn^{2+} sequestration.[12] Clioquinol, a proposed therapeutic agent for Alzheimer's disease, is suggested to suppress apoptosis by chelating and facilitating the redistribution of excess copper and zinc in neurons.[13] The details of the Zn^{2+} binding sites must be taken into account for the design of more specific chelating agents. Secondly, synthetic caspase inhibitors currently in clinical trials target the active site Cys of caspases.[14] Hurdles to overcome in this approach are the peptidic nature of the inhibitors and their promiscuity with regard to other cysteine proteases. Based on the insights gained from this study, the catalytic His can be considered a novel target for the small-molecule based inhibition of caspases. For example, Co^{3+} complexes that selectively bind to histidine could be considered as templates for drug design.[15]

An understanding of the bioinorganic chemistry of apoptosis, including the details of the role of metal ions in one of life's fundamental processes, cell death, is essential to maximizing drug interventions and is crucial for the improvement of such therapies.

Received: December 23, 2013
Published online: March 18, 2014

Keywords: apoptosis · caspases · density functional calculations · enzyme kinetics · zinc

[1] P. Fuentes-Prior, G. S. Salvesen, *Biochem. J.* **2004**, *384*, 201 – 232.
[2] A. Q. Truong-Tran, L. H. Ho, F. Chai, P. D. Zalewski, *J. Nutr.* **2000**, *130*, 1459S – 1466S.
[3] A. R. Mufti, E. Burstein, R. A. Csomos, P. C. F. Graf, J. C. Wilkinson, R. D. Dick, M. Challa, J. Son, S. B. Bratton, G. L. Su, G. J. Brewer, U. Jakob, C. S. Duckett, *Mol. Cell* **2006**, *21*, 775 – 785.
[4] a) D. K. Perry, M. J. Smyth, H. R. Stennicke, G. S. Salvesen, P. Duriez, G. G. Poirier, Y. A. Hannun, *J. Biol. Chem.* **1997**, *272*, 18530 – 18533; b) H. R. Stennicke, G. S. Salvesen, *J. Biol. Chem.* **1997**, *272*, 25719 – 25723; c) K. L. Huber, J. A. Hardy, *Protein Sci.* **2012**, *21*, 1056 – 1065.
[5] a) W. Maret, C. Jacob, B. L. Vallee, E. H. Fischer, *Proc. Natl. Acad. Sci. USA* **1999**, *96*, 1936 – 1940; b) W. Maret, *Biometals* **2013**, *26*, 197 – 204.
[6] E. M. Velazquez-Delgado, J. A. Hardy, *J. Biol. Chem.* **2012**, *287*, 36000 – 36011.
[7] a) M. Kyoung, S. Y. Kim, H. Seok, I. Park, M. Lee, *Biochim. Biophys. Acta Proteins Proteomics* **2002**, *1598*, 74 – 79; b) I. Park, H. R. Moon, H. Seok, M. Lee, *Biochim. Biophys. Acta Proteins Proteomics* **2004**, *1700*, 5 – 9.
[8] S. Lampa-Pastirk, R. C. Lafuente, W. F. Beck, *J. Phys. Chem. B* **2004**, *108*, 12602 – 12607.
[9] G. Parkin, *Chem. Rev.* **2004**, *104*, 699 – 767.
[10] T. Fukuyama, K. Kuchitsu, Y. Tamaru, Z. Yoshida, I. Tabushi, *J. Am. Chem. Soc.* **1971**, *93*, 2799 – 2800.
[11] M. Babor, H. M. Greenblatt, M. Edelman, V. Sobolev, *Proteins Struct. Funct. Bioinf.* **2005**, *59*, 221 – 230.
[12] Q. P. Peterson, D. R. Goode, D. C. West, K. N. Ramsey, J. J. Y. Lee, P. J. Hergenrother, *J. Mol. Biol.* **2009**, *388*, 144 – 158.
[13] A. I. Bush, R. E. Tanzi, *Neurotherapeutics* **2008**, *5*, 421 – 432.
[14] T. O'Brien, S. D. Linton, *Design of Caspase Inhibitors as Potential Clinical Agents*, CRC, Boca Raton, FL, **2009**, pp. 161 – 287.
[15] A. Y. Louie, T. J. Meade, *Proc. Natl. Acad. Sci. USA* **1998**, *95*, 6663 – 6668.